

# Dynamic-Change Laws of the Porosity and Permeability of Low- to Medium-Rank Coals under Heating and Pressurization Treatments in the Eastern Junggar Basin, China

Gang Wang<sup>1,2</sup>, Yong Qin<sup>1\*</sup>, Jian Shen<sup>1</sup>, Shuyuan Chen<sup>1</sup>, Beibei Han<sup>3</sup>, Xiaoting Zhou<sup>4</sup>

1. Key Laboratory of Coalbed Methane Resources and Reservoir Formation Process of the Ministry of Education,  
China University of Mining and Technology, Xuzhou 221116, China

2. Key Laboratory of Resource Survey and Research of Hebei Province, Hebei University of Engineering, Handan 056038, China

3. China Chemical Geology and Mine Bureau, Beijing 100013, China

4. Institute of Technology, East China Jiaotong University, Nanchang 330100, China

<sup>1</sup>D Gang Wang: <https://orcid.org/0000-0002-1008-3781>; <sup>1</sup>D Yong Qin: <https://orcid.org/0000-0002-7478-8828>

**ABSTRACT:** Deep coalbed methane exists in high-temperature and high-pressure reservoirs. To elucidate the dynamic-change laws of the deep coal reservoir porosity and permeability characteristics in the process of coalbed methane production, based on three pieces of low- to medium-rank coal samples in the eastern Junggar Basin, Xinjiang, we analyse their mercury-injection pore structures. We measured the porosity and permeability of the coal samples at various temperatures and confining pressures by high-temperature and confining pressure testing. The results show that the porosity of a coal sample decreases exponentially with increasing effective stress. With increasing temperature, the initial porosity increases for two pieces of relatively low-rank coal samples. The increased rate of porosity decreases with increasing confining pressure. With increasing temperature, the initial porosity of a relatively high-rank coal sample decreases, and the rate of change of the porosity become faster. An exponential relationship exists between the porosity and permeability. With increasing coal rank, the initial porosity and permeability decrease. The change rate of the permeability decreases with increasing porosity.

**KEY WORDS:** high-temperature and confining pressure, coalbed methane reservoir, porosity, permeability, dynamic change.

## 0 INTRODUCTION

China is rich in deep coalbed methane resources. The geological resource of coalbed methane is  $11.93 \times 10^{12} \text{ m}^3$  between 1 500–2 000 m in depth, accounting for 32.4% of the total resources above 2 000 m, which are mainly distributed in the northwestern Junggar Basin and the northern regions of the Ordos Basin and Qinshui Basin (Liu et al., 2009). In the Junggar Basin, there is a  $3.87 \times 10^{12} \text{ m}^3$  coalbed methane resource that is shallower than 2 000 m and a  $1.57 \times 10^{12} \text{ m}^3$  coalbed methane resource at a reservoir depth between 1 500 and 2 000 m. The favourable area is mainly distributed in the Fukang and Wucaiwan areas (Li et al., 2012). It is known that with increasing buried depth, the permeability of a coal seam is reduced. This is disadvantageous for mining deep coalbed methane resources (Qin et al., 2012; Cui and Bustin, 2005). However, successful examples exist. For example, at the start of this century, the United States performed a co-mining experiment of

deep coalbed gas and low-permeability sandstone gas in the White River uplift of the Piceance Basin. The buried depth of the target coal seam was 1 560–2 561 m, and single-well gas production of 65 wells is stable at approximately  $10\ 890 \text{ m}^3/\text{d}$ , 60% of which is derived from the coal seam (Olson et al., 2002; Nelson et al., 2000). There are 30 coalbed gas wells in three Rocky Mountain basins that produce from reservoir depths greater than 1 370 m. The cumulative gas production through year-end 2001 from these 30 deep coalbed gas wells totals  $1.12 \times 10^{15} \text{ m}^3$  (Nelson, 2003). In the eastern Junggar Basin, we have tested coal seam gas at the Jurassic formation in 1993. We obtain 2 000–4 000  $\text{m}^3/\text{d}$  airflow (Cui et al., 2007). From 2005 to 2007, using an abandoned conventional oil and gas well, we performed fracturing and drainage in a deep coal seam, the depth of which is 2 567–2 583 m. The maximum production capacity is  $6\ 500 \text{ m}^3/\text{d}$  (Qin et al., 2012). The engineering practice proves that there is still a large recoverable potential for deep coalbed methane under the conditions of high temperature and high pressure.

It is difficult to measure the dynamic-change law of coal seam permeability in the coalbed methane mining process directly. Studying the relationship between the coal porosity, permeability and formation temperature and pressure is an indirect way to predict the variation of deep coal seam permeability.

The relationship between the porosity and permeability of

\*Corresponding author: [yongqin@cumt.edu.cn](mailto:yongqin@cumt.edu.cn)

© China University of Geosciences and Springer-Verlag GmbH Germany, Part of Springer Nature 2018

Manuscript received October 15, 2016.

Manuscript accepted March 9, 2017.

coal reservoirs has been investigated. Many of them are the empirical equation (Moosavi et al., 2014; McKee et al., 1988; Reiss, 1980; Carman, 1956). Palmer and Mansoori (1998, 1996) deduced a simplified formula for the porosity and permeability of coal rock. Permeability is proportional to the third power of porosity, which is widely used in coal reservoir numerical simulations. However, the relationship between the porosity and permeability of coal reservoirs under high-temperature and high-pressure conditions has not been reported.

Many studies have been performed, both in China and globally, on the relationship between the coal rock porosity, permeability and temperature and pressure. McKee et al. (1988), Palmer (2010, 2009) discussed the deep coal rock porosity and pore compressibility with dynamically changing effective stress. However, the deep coal rock pore compressibility under high-temperature and high-pressure conditions has been only infrequently reported. Niu et al. (2014), Yin et al. (2013), Perea et al. (2012), Qin et al. (2012), Jasinge et al. (2011), Harpalani and Mopherson (1984), and Somerton et al. (1975) investigated the relationship between the coal permeability and effective stress, pore pressure and temperature. A comprehensive formula relating the effective stress, permeability and temperature was deduced (Pan and Connell, 2012; Li et al., 2009; Shi and Durucan, 2004; Cheng et al., 1998; Seidle et al., 1992). Shen (2011) observed the temperature effect on the seepage ability of coal rock which is controlled by the coal rank. Heat can improve the pore structure of the low and medium

rank coals with a large amount of micropores generated during the heating process (Cai et al., 2014). The dynamic-change laws of porosity and permeability of low- to medium-rank coals under heating and pressurization treatments are less reported.

In this paper, we built on results from the literature by performing simulation experiments on the coal rock permeability under high temperature and confining pressure. We also analysed the evolution law of the low-medium rank coal rock porosity and permeability under various temperature and pressure conditions. The coal samples were obtained from the eastern Junggar Basin in Xinjiang, China. We propose a quantitative, characteristic equation that can be used for predicting the porosity and permeability characteristics of deep coal reservoirs.

## 1 COAL SAMPLES AND EXPERIMENTAL METHOD

The coal samples used for experiment were collected from the Laojunmiao, Tianlong and Xiaoxigou mines, which are distributed in the eastern Junggar Basin, Xinjiang, China. The Laojunmiao and Tianlong coal samples are from the Xishanyao Formation, Middle Jurassic series. The Xiaoxigou coal sample is from the Badaowan Formation, Lower Jurassic series. The raw coal blocks all consisted of a side length of more than 200 mm and collected from the new working faces of the coal mines. All coal blocks were immediately wrapped with black polyethylene bags once collected, and then carried to CBM laboratory for sample preparations and coal analyses before the coal porosity and permeability tests. The collected raw coal blocks were drilled

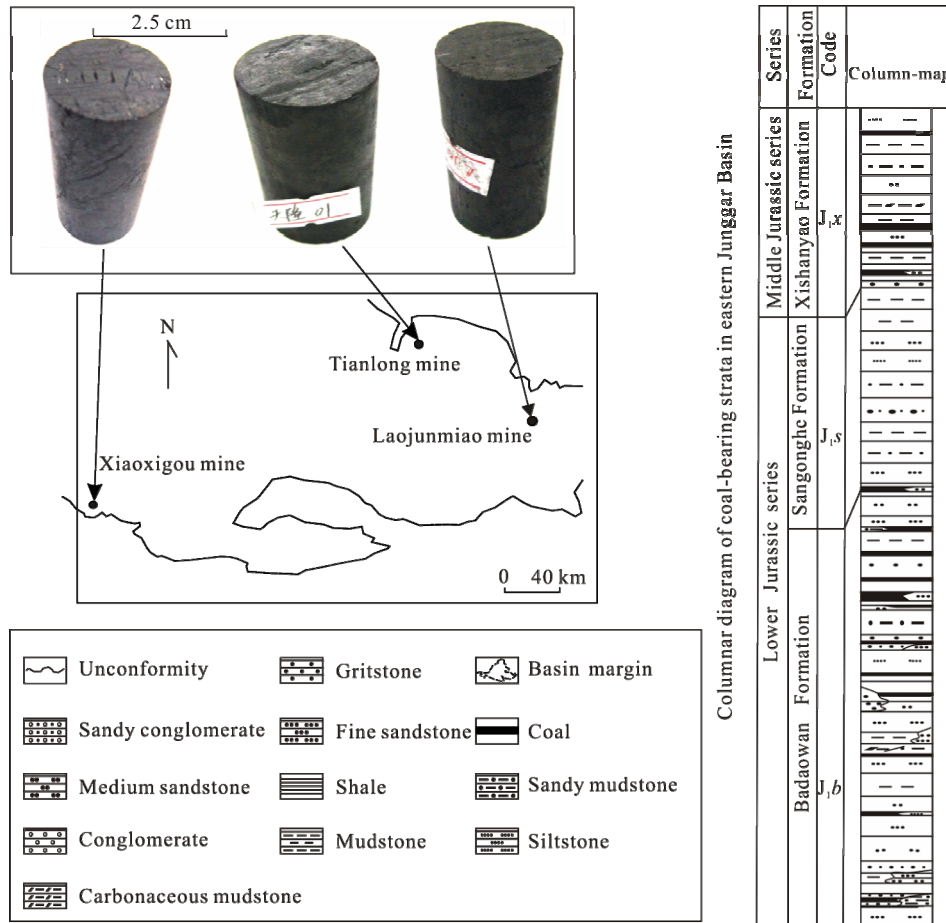


Figure 1. Collection location and macroscopic characteristics of the coal sample.

**Table 1** Test results for the basic properties of the coal samples

| Number | Producing area  | Position         | $R_o$ <sub>max</sub> <sup>a</sup><br>(%) | Proximate analysis (%) |                       |                        | Coal macerals (%) |                  |                  |
|--------|-----------------|------------------|--|------------------------|-----------------------|------------------------|-------------------|------------------|------------------|
|        |                 |                  |  | $M_{ad}$ <sup>b</sup>  | $A_{ad}$ <sup>b</sup> | $V_{daf}$ <sup>b</sup> | $V$ <sup>c</sup>  | $I$ <sup>c</sup> | $E$ <sup>c</sup> |
| ZD01   | Laojunmiao mine | J <sub>1</sub> X | 0.62                                     | 9.43                   | 2.98                  | 29.99                  | 32.43             | 61.56            | 1.2              |
| ZD02   | Tianlong mine   | J <sub>1</sub> X | 0.81                                     | 10.31                  | 3.6                   | 28.52                  | 28.94             | 63.67            | 2.57             |
| ZD03   | Xiaoxigou mine  | J <sub>1</sub> b | 0.93                                     | 3.25                   | 2.19                  | 25.19                  | 43.61             | 54.76            | 0.66             |
|        |                 |                  |  |                        |                       |                        |                   |                  | 0.98             |

<sup>a</sup> Mean maximum vitrinite reflectance in oil. <sup>b</sup>  $V_{daf}$ ,  $M_{ad}$ , and  $A_{ad}$  represent the volatile yield of the dry ash-free basis, moisture content of the air-dried basis and ash yield of the dry ash-free basis, respectively. <sup>c</sup>  $V$ ,  $I$ , and  $E$  represent the volume percentages of vitrinite, inertinite and liptinite in the coal maceral composition, respectively.  $M$  is the volume percentage of minerals on a dry basis.

into cylindrical coal samples with a diameter of 25 mm and height of 50 mm along the bedding plane from the raw coal blocks, providing coal samples for the coal porosity and permeability tests. The coal samples of column which used in the porosity and permeability test were stored and sealed in polyethylene film wrap. Meanwhile, the cut offs from coal column ends were collected and divided into two part. One part was crushed and ground to less than 60–80 mesh (about 0.178–0.25 mm) for coal proximate and petrology analyses as shown in Table 1. Another part was broken into particle sizes that are greater than 2 mm for mercury-injection experiment (Shen et al., 2011).

Among them, the Laojunmiao and Tianlong coal samples exhibit few endogenous fractures by visual inspection. The Xiaoxigou coal sample has a larger number of endogenous fractures (Fig. 1). The vitrinite maximum reflectance of the Laojunmiao coal sample is 0.62%, characterising it as jet coal; the vitrinite maximum reflectivity of the Tianlong coal sample is 0.81%, characterising it as gas coal; and the vitrinite maximum reflectivity of the Xiaoxigou coal sample is 0.93%, characterising it as fat coal. The ash yield of the three coal samples is low. For the microstructural composition of the three coal samples, the inertinite content is highest, the vitrinite content is lower, and the liptinite and mineral content are even lower (Table 1).

The mercury-injection experiment used an Autopore IV9510 porosity-measuring instrument made in the U.S.A. The mercury-injection pressure ranges from 0 to 414 MPa. The measurable pore diameter is greater than 3 nm. Putting the coal samples into the sample chamber and increasing the pressure on the coal sample gradually according to the procedure, we obtain the mercury-injection and mercury-ejection curves, porosity, pore volume, pore structure and specific surface area.

The high-temperature and confining-pressure simulation experiments used columnar coal samples, which had diameters of 25 mm and heights of 50 mm (Fig. 1). The experimental device is a high-temperature and confining-pressure tester GWFY-01 made in China. According to the previous studies, the buried depth of coal seam of Badaowan Formation in this region is in the range of 900–3 300 m. The buried depth of coal seam of Xishanyao Formation is in the range of 600–2 900 m. The average effective stress gradient of coal-bearing strata is 1.025 MPa/100 m in eastern Junggar Basin (Wang et al., 2014). The effective stress is 30.75 MPa when buried depth is 3 000 m. The modern average geothermal gradient in Junggar Basin is 2.55 °C/100 m. Deducting the thermostatic temperature (15 °C), the temperature is 91.5 °C when buried depth is 3 000 m (Sang et al., 2003; Zhou and Pan, 1992). According to the buried depth, for-

mation pressure and formation temperature of the coal seam in the eastern Junggar Basin, we designed 30, 50, 70 and 90 °C as the experimental temperatures. For each temperature, we designed 12 confining pressure points (2, 3.5, 5, 8, 11, 15, 19, 23, 27, 31, 35 and 40 MPa). The test medium is nitrogen with a purity of 99.999%. Measuring the permeability and porosity simultaneously, we can test the porosity and permeability of the coal samples in identical temperature and pressure settings.

The whole test process carried out according to the procedure. The test is composed of two stages. After putting core into the holder and applied a fixed confining pressure and temperature, the porosity would be tested first. Without considering the nitrogen adsorption, according the Boyle law and the Darcy law, the porosity and permeability of coal sample will be tested according to method of core routine analysis SY/T 5336-1996 (China National Petroleum and Gas Corporation Oil and Gas Field Development Professional Standardization Committee, 1996) and the porosity and permeability measurement of core in net confining stress SY/T 6385-1999 (Shengli Petroleum Administration Institute of Geological Sciences, 1999). Effective stress is the difference between confining pressure and fluid pressure. Due to the nitrogen gas fluid pressure is less than 0.5 MPa, and decreasing during the testing process, the effective stress cannot be obtained accurately. We focus on the relationships between confining pressure and porosity, porosity and permeability.

## 2 EXPERIMENTAL RESULTS AND ANALYSES

### 2.1 Porosity Characteristics

Low rank coal has undeveloped cleats and relatively large matrix porosity, mainly existing as primary porosity. With increasing coal evolution, the micropores and pore specific surface area increase gradually, and the macropores and mesopores decrease (Chen, 2007). The pore volume proportion of the Laojunmiao coal sample is 63.37% macropores and mesopores. The specific surface area proportion of the macropores and mesopores is only 7%. The mercury-intrusion porosity is 17.91%. The average diameter of the pore is 21.7 nm. The pore volume proportion of the Tianlong coal sample is 92.94% macropores and mesopores. The specific surface area proportion of the macropores and mesopores is only 25.5%. The mercury-intrusion porosity is 28.11%. The average diameter of the pore is 53.3 nm. The pore volume proportion of the Xiaoxigou coal sample is 33.46% macropores and mesopores. The specific surface area proportion of macropores and mesopores is only 4.1%. The mercury-intrusion porosity is 9.19%. The average diameter of the pores is 11 nm (Tables 2, 3).

Song (2004) considered that the pores with diameters greater than 100 nm provided a diffusion-seepage-migration channel for coalbed methane and determined the difficulty of fluid seepage in a coal reservoir. In this article, the diameter of the seepage pores is believed to be greater than 100 nm. The mercury-injection porosities of the Laojunmiao and Tianlong coal samples are larger. The pore volume proportion of macropores and mesopores is large, and the median diameter of the pore volume is large. These characteristics are beneficial for coalbed methane diffusion and storage. On the other hand, the mercury-injection porosity of the Xiaoxigou coal sample is smaller. The pore volume proportion of macropores and mesopores is smaller, and the median diameter of the pore volume is smaller. However, they can develop small macrofractures that are beneficial for coalbed methane diffusion. The pore specific surface area of the transition pores and micropores in the three coal samples is larger (Fig. 2). This is beneficial for absorbing coalbed methane (Li et al., 2013; Gürdal and Yalçın, 2001).

The rise rate of the mercury-injection curve of the Laojunmiao coal sample is smooth, and the pore size is well distributed. The efficiency of the mercury ejection is 24.54%. The connectivity of the pores is poor (Fig. 3a); the mercury-injection curve of the Tianlong coal sample exhibits an "S" shape. This is related to the large pore volume of the macropores and mesopores. The

efficiency of mercury ejection is 13.7%. For a mercury-injection pressure of 100–1 000 psi, the mercury-injection curve rises quickly. This illustrates that bottleneck pores exist and that the connectivity of the pores is poor (Fig. 3b). The mercury-ejection curve of the Xiaoxigou coal sample rises rapidly when the injection pressure increases. This is related to the large pore volume of the transition pores. The efficiency of mercury ejection is 58.5%, and the pore connectivity is good (Fig. 3c).

## 2.2 Permeability Characteristics

The porosity decreases exponentially with increasing confining pressure. When the temperature is different, the change trends become different. The change trends of the Laojunmiao and Tianlong coal samples are similar. The initial porosity increases with increasing temperature. We believe that, with increasing temperature, the plasticity of the coal is enhanced. When the confining pressure is small, the opening degree of the pores and the expansion of the coal matrix are larger. The coal rock expands outward. This increases the porosity of the coal (Li et al., 2009). As the temperature and confining pressure increase, the change rate of the Laojunmiao and Tianlong coal samples slows. We believe that pores are more difficult to compress at low temperature. Because the initial porosities of

**Table 2** Pore volume distribution for the coal sample

| Producing area  | Pore volume ( $10^{-4} \text{ cm}^3/\text{g}$ ) |       |       |       |       | Ratio of the pore volume (%) |           |           |           |
|-----------------|---|-------|-------|-------|-------|------------------------------|-----------|-----------|-----------|
|                 | $V_1$   | $V_2$ | $V_3$ | $V_4$ | $V_t$ | $V_1/V_t$                    | $V_2/V_t$ | $V_3/V_t$ | $V_4/V_t$ |
| Laojunmiao mine | 274   | 385   | 327   | 54    | 1 040 | 26.35                        | 37.02     | 31.44     | 5.19      |
| Tianlong mine   | 1 209   | 1 200 | 139   | 44    | 2 592 | 46.64                        | 46.30     | 5.36      | 1.70      |
| Xiaoxigou mine  | 32  | 147   | 290   | 66    | 535   | 5.98                         | 27.48     | 54.21     | 12.34     |

$V$ ,  $V_1$ ,  $V_2$ ,  $V_3$ ,  $V_4$ , and  $V_t$  represent the pore volume, macropore volume ( $\phi > 1000 \text{ nm}$ ), mesopore volume ( $1000 \text{ nm} > \phi > 100 \text{ nm}$ ), transition pore volume ( $100 \text{ nm} > \phi > 10 \text{ nm}$ ), micropore volume ( $10 \text{ nm} > \phi > 7.2 \text{ nm}$ ) and total pore volume, respectively.

**Table 3** Distribution of the pore specific surface area

| Producing area  | Pore specific surface area ( $\text{m}^2/\text{g}$ ) |       |       |       | Pore specific surface area ratio (%) |             |             |             |             |
|-----------------|--|-------|-------|-------|--------------------------------------|-------------|-------------|-------------|-------------|
|                 | $S_1$  | $S_2$ | $S_3$ | $S_4$ | $S_t$                                | $S_1 / S_t$ | $S_2 / S_t$ | $S_3 / S_t$ | $S_4 / S_t$ |
| Laojunmiao mine | 0.046  | 0.522 | 5.147 | 2.42  | 8.135                                | 0.6         | 6.4         | 63.3        | 29.7        |
| Tianlong mine   | 0.277  | 1.111 | 2.056 | 2.012 | 5.456                                | 5.1         | 20.4        | 37.7        | 36.9        |
| Xiaoxigou mine  | 0.001  | 0.325 | 4.491 | 3.049 | 7.866                                | 0           | 4.1         | 57.1        | 38.8        |

$S$ ,  $S_1$ ,  $S_2$ ,  $S_3$ ,  $S_4$ , and  $S_t$  represent the pore specific surface area, macropore specific surface area ( $\phi > 1000 \text{ nm}$ ), mesopore specific surface area ( $1000 \text{ nm} > \phi > 100 \text{ nm}$ ), transition pore specific surface area ( $100 \text{ nm} > \phi > 10 \text{ nm}$ ), micropore specific surface area ( $10 \text{ nm} > \phi > 7.2 \text{ nm}$ ) and total pore specific surface area, respectively.

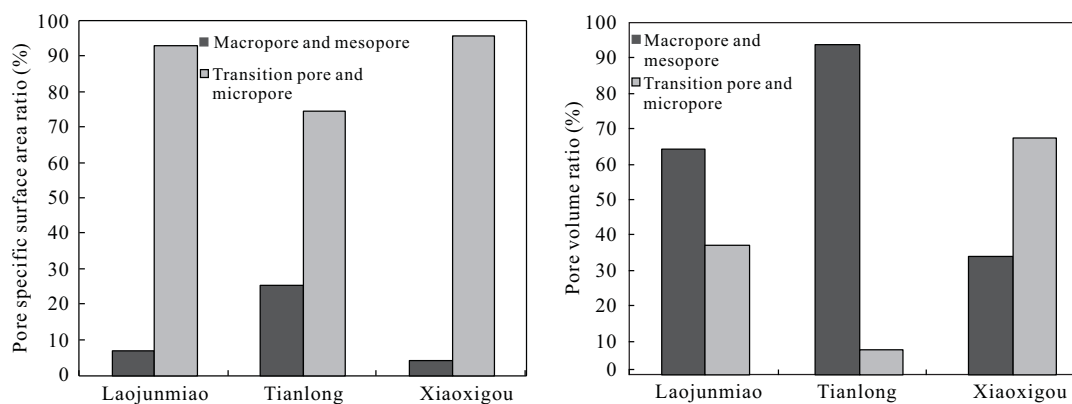


**Figure 2.** Ratio distribution of pore specific surface area and pore volume.



initial porosity and initial permeability decrease. The rate of change of the permeability with the porosity decreases (Fig. 7).

Because the initial porosity and permeability of low-medium rank coal is larger, the porosity and permeability of deep coal seams under high temperatures and confining pressures are also promising. Nelson and Kibler (1994) and Feng et al. (2008) believed that the following relationship between the porosity and permeability exists, which is generally obtained by core analysis

$$K=a \exp(b\varphi) \quad (1)$$

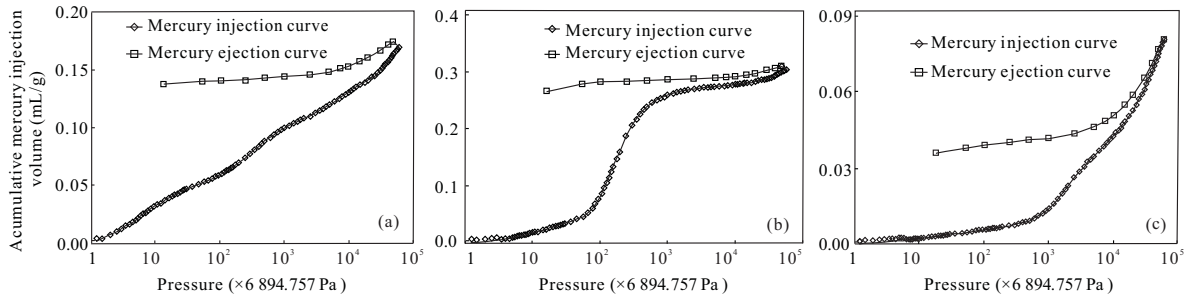


**Figure 3.** Mercury injection curve of Laojunmiao (a), Tianlong (b) and Xiaoxigou (c) coal samples.

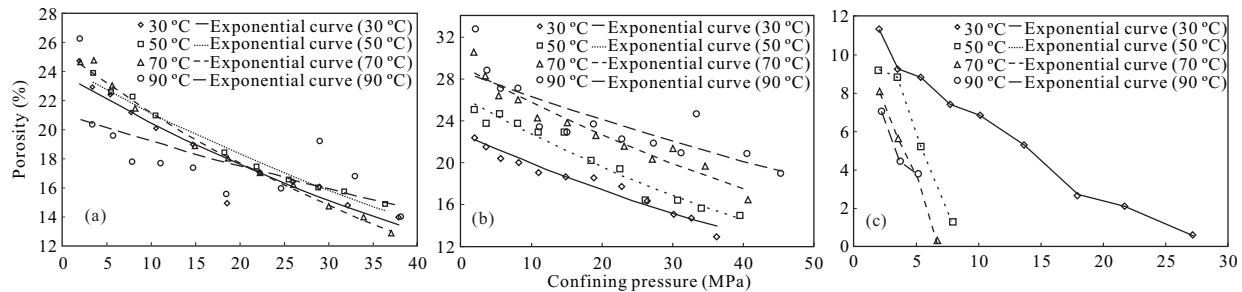


**Figure 4.** Porosity changes with the overburden pressure for the Laojunmiao (a), Tianlong (b) and Xiaoxigou (c) coal samples.

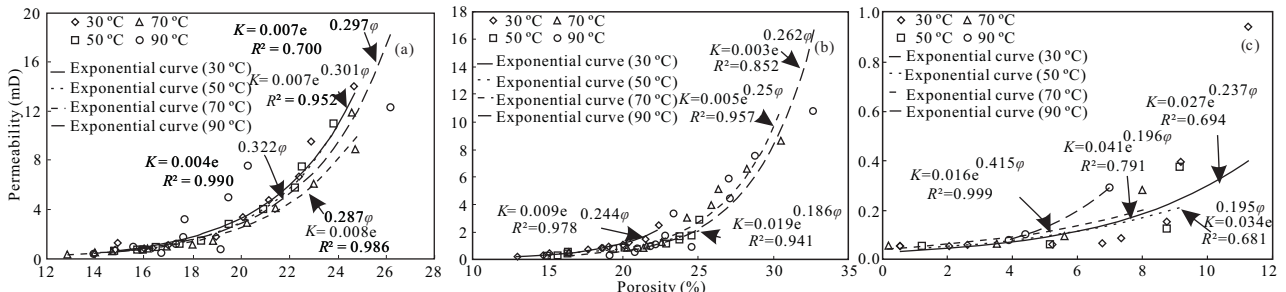


**Figure 5.** Relationship between the porosity and permeability of the the Laojunmiao (a), Tianlong (b) and Xiaoxigou (c) coal samples.

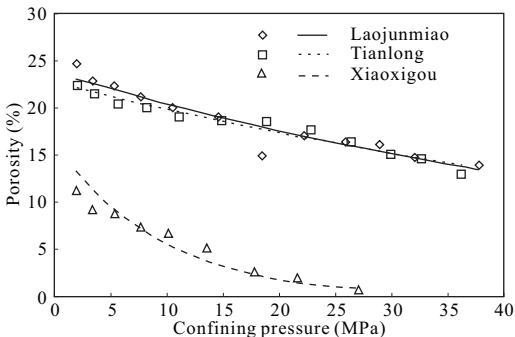


**Figure 6.** Porosity changes with the overlying pressure diagram of three coal samples.

where  $K$  is the permeability;  $\varphi$  is the porosity; and  $a$  and  $b$  are constant. The fitting relationships between the porosity and the permeability of the Laojunmiao coal sample under various temperatures and pressures are

$$\text{when } 30^\circ\text{C}, K=0.0078 \exp(0.3015\varphi), R^2=0.952 \quad (2)$$

$$\text{when } 50^\circ\text{C}, K=0.0047 \exp(0.3228\varphi), R^2=0.990 \quad (3)$$

$$\text{when } 70^\circ\text{C}, K=0.008 \exp(0.2878\varphi), R^2=0.986 \quad (4)$$

**Figure 7.** Relationship between the porosity and permeability of the three coal samples.

$$\text{when } 90^\circ\text{C}, K=0.0075 \exp(0.2976\phi), R^2=0.700 \quad (5)$$

The fitting relationships between the porosity and the permeability of the Tianlong coal sample under various temperatures and pressures are

$$\text{when } 30^\circ\text{C}, K=0.009 \exp(0.2446\phi), R^2=0.978 \quad (6)$$

$$\text{when } 50^\circ\text{C}, K=0.0202 \exp(0.185\phi), R^2=0.941 \quad (7)$$

$$\text{when } 70^\circ\text{C}, K=0.0053 \exp(0.2497\phi), R^2=0.957 \quad (8)$$

$$\text{when } 90^\circ\text{C}, K=0.0032 \exp(0.2622\phi), R^2=0.852 \quad (9)$$

The fitting relationship between the porosity and the permeability of the Xiaoxigou coal sample under various temperatures and pressures are

$$\text{when } 30^\circ\text{C}, K=0.0275 \exp(0.2375\phi), R^2=0.694 \quad (10)$$

$$\text{when } 50^\circ\text{C}, K=0.0348 \exp(0.1957\phi), R^2=0.681 \quad (11)$$

$$\text{when } 70^\circ\text{C}, K=0.0417 \exp(0.1967\phi), R^2=0.791 \quad (12)$$

$$\text{when } 90^\circ\text{C}, K=0.016 \exp(0.4153\phi), R^2=0.999 \quad (13)$$

The  $a$  is the value of the permeability when the coal sample porosity is zero, and it reflects the connectivity of the pores and cracks. The  $b$  is the attenuation coefficient of the permeability when the porosity decreases. With increasing coal rank, the range of the change in  $a$  and  $b$  increases, and the rate of change increases. The range of the change in the Xiaoxigou coal sample is the largest, and that of the Laojunmiao coal sample is the smallest. With increasing coal rank, the number of seepage throats increases, and cracks develop gradually. These throats and cracks provide seepage channels. The seepage ability of a crack is greater than that of a pore throat. With increasing confining pressure, the porosity of crack decreases quickly (Fig. 5). With increasing coal rank, the change range of  $a$  and  $b$  increase. With increasing temperature, the internal energy of the gas increases, which improves the permeability (Cheng et al., 1998). When the temperature is too high, the coal crack seepage channel is reduced because of the rock thermal expansion. Thus, with increasing temperature, the  $a$  value increases first and then decreases. The attenuation coefficient ( $b$ ) decreases first and then increases (Figs. 8, 9). The microcracks of coal, especially the

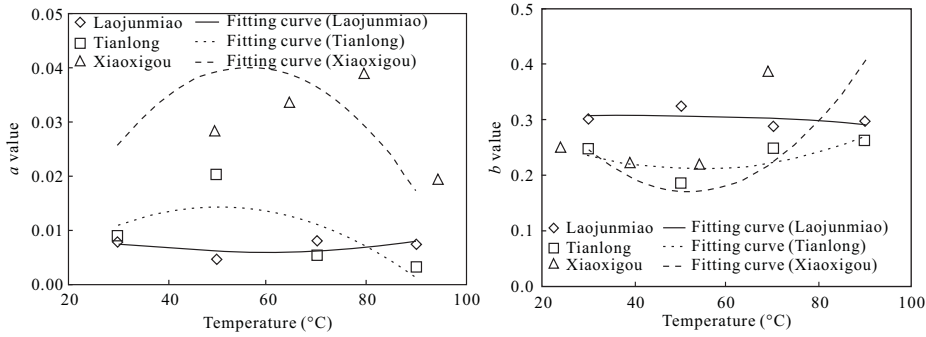


Figure 8. Plots of  $a$  and  $b$  values vs. temperature.

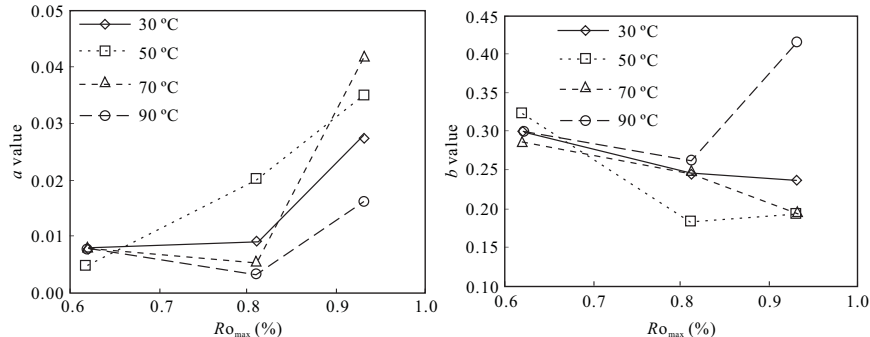


Figure 9. Plots of  $a$  and  $b$  values vs. coal rank.

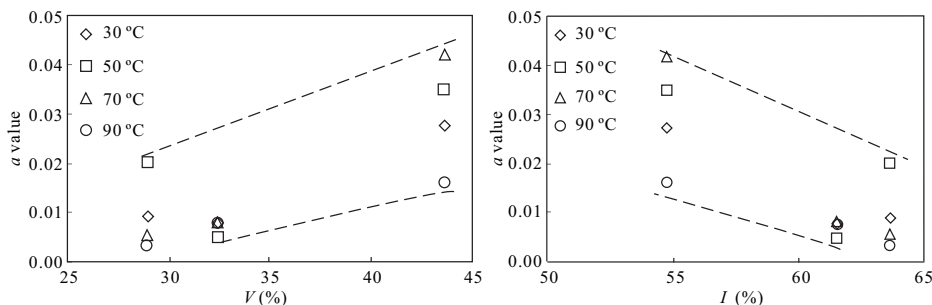


Figure 10. Plots of  $a$  values vs. volume percentages of vitrinite and inertinite.

endogenous fractures are closely related to coal petrology characteristics (Tang et al., 2014; Lan et al., 2012).

The increasing volume percentage of vitrinite is benefit for the development of endogenous fractures. The  $a$  value showed a rising trend. The increasing volume percentage of inertinite goes against the development of endogenous fractures. The  $a$  value showed a falling trend (Fig. 10). There are many factors that influence the permeability, such as the length and width of fracture, pore radius, pore connectivity, pore ratio and pore tortuosity, porosity, mineral filling (He and Yang, 2005; Laubach et al., 1998). The heterogeneity of coal leads to empiricism of the prediction formula permeability. Predecessors had obtained many empirical formulas in the study of the relationship between the effective stress and porosity, porosity and permeability which has been described in the "Introduction". But the empirical exponential relationship between porosity and permeability is suit for the results of experiment in this paper. The fitting degree is high.

### 3 CONCLUSIONS

(1) Using mercury-injection experiments, we can conclude that the mercury-injection porosity of the Laojunmiao and Tianlong coal samples is larger and that the proportion of macropores and mesopores is larger. This is beneficial for the diffusion and storage of coalbed methane. The mercury-injection porosity of the Xiaoxigou coal sample is small, and the proportion of transition pores and micropores is larger. The sum of the micropore and transition pore specific surface areas of the three coal samples is large, which is beneficial for adsorption of coalbed methane.

(2) From the results of high-temperature and confining-pressure experiments, we can conclude that the porosity decreases exponentially as the confining pressure increases. The initial porosity of the Laojunmiao and Tianlong coal samples increases with increasing temperature. The rate of change of the porosity decreases as the confining pressure increases. The initial porosity of the Xiaoxigou coal sample decreases with increasing temperature. The rate of change of the porosity increases with increasing confining pressure. With increasing coal rank, the initial porosity decreases. With increasing confining pressure, the reduction rate of the porosity accelerates. The relationship between the porosity and the permeability is exponential. With increasing temperature and porosity, the permeability rate of change of the Laojunmiao and Tianlong coal samples slows. At the same larger porosity, with increasing temperature, the permeability decreases. The Xiaoxigou coal sample change trend is opposite. With increasing temperature and porosity, the rate of change of the permeability accelerates. At the same larger porosity, the permeability increases with increasing temperature. With increasing coal rank, the initial porosity and initial permeability decrease. The rate of change of the permeability decreases with increasing porosity.

(3) With increasing coal rank, the range of the change in  $a$  and  $b$  increases. The  $a$  and  $b$  values of the Laojunmiao coal sample change slowly with increasing temperature. Although the proportion of macropores and mesopores is large, the number of seepage throats is small and their connectivity is poor. With increasing coal rank, the number of seepage throats in-

creases and cracks develop gradually. The  $a$  values of the Tianlong and Xiaoxigou coal samples increase first and then decrease, and the attenuation coefficient ( $b$  value) decreases first and then increases. The increasing volume percentage of vitrinite is benefit for the development of endogenous fractures. The  $a$  value showed a rising trend. The increasing volume percentage of inertinite goes against the development of endogenous fractures. The  $a$  value showed a falling trend.

### ACKNOWLEDGMENTS

This research was funded by the National Natural Science Fundation of China (Nos. 41672149, 41302131, 41362009), the Key Project of the National Natural Science Foundation of China (No. 41530314), the Scientific Research Foundation of the Key Laboratory of Coalbed Methane Resources and Reservoir Formation Process of the Ministry of Education, China University of Mining and Technology, (No. 2017-001), the National Science and Technology Major Project of the Ministry of Science and Technology of China (Nos. 2016ZX05044-002, 2011ZX05033, 2011ZX05034), and the Fundamental Research Funds for the Central Universities (No. 2012QNB32). The final publication is available at Springer via <https://doi.org/10.1007/s12583-017-0908-4>.

### REFERENCES CITED

- Cai, Y. D., Liu, D. M., Pan, Z. J., et al., 2014. Pore Structure of Selected Chinese Coals with Heating and Pressurization Treatments. *Science China Earth Sciences*, 57(7): 1567–1582. <https://doi.org/10.1007/s11430-014-4855-y>
- Carman, P. C., 1956. Flow of Gases through Porous Media. Butterworths Scientific Publications, London. 12–33
- China National Petroleum and Gas Corporation Oil and Gas Field Development Professional Standardization Committee, 1996. Method of Core Routine Analysis, SY/T 5336-1996. China National Petroleum Corporation, Beijing. 1–79 (in Chinese)
- Chen, Z. H., 2007. Key Controlling Factors Comparison between High and Low Rank CBM Reservoir Formation: [Dissertation]. University of the Chinese Academy of Sciences, Guangzhou. 31 (in Chinese with English Abstract)
- Cheng, D. R., Chen, H. Y., Xian, X. F., et al., 1998. Experiments on the Affection of Temperature on Permeability Coefficient of Coal Samples. *Coal Engineer*, 1: 13–16 (in Chinese with English Abstract)
- Cui, S. H., Liu, H. L., Wang, B., 2007. Trapping Characteristics of Coalbed Methane in Low-Rank Coal of Zhungaer Basin. *Geoscience*, 21(4): 719–724 (in Chinese with English Abstract)
- Cui, X. J., Bustin, R. M., 2005. Volumetric Strain Associated with Methane Desorption and Its Impact on Coalbed Gas Production from Deep Coal Seams. *AAPG Bulletin*, 89(9): 1181–1202. <https://doi.org/10.1306/05110504114>
- Feng, M. S., Yuan, S. Y., Zhao, L. M., 2008. Permeability Up-Scaling Method Based on the Relationship between Porosity and Permeability. *Xinjiang Petroleum Geology*, 29(4): 502–503 (in Chinese with English Abstract)
- Gürdal, G., Yalçın, M. N., 2001. Pore Volume and Surface Area of the Carboniferous Coals from the Zonguldak Basin (NW Turkey) and Their Variations with Rank and Maceral Composition. *International Journal of Coal Geology*, 48(1): 133–144. [https://doi.org/10.1016/S0166-5162\(01\)00051-9](https://doi.org/10.1016/S0166-5162(01)00051-9)
- Harpalani, S., MoPherson, M. J., 1984. The Effect of Gas Evacuation on Coal Permeability Test Specimens. *International Journal of Rock Mechanics and Mining Sciences*, 21(3): 161–164. [https://doi.org/10.1016/0148-9062\(84\)91534-1](https://doi.org/10.1016/0148-9062(84)91534-1)
- He, Y. L., Yang, L. Z., 2005. Mechanism of Effects of Temperature and Effective

- Stress on Permeability of Sandstone. *Chinese Journal of Rock Mechanics and Engineering*, 24(14): 2420–2427 (in Chinese with English Abstract)
- Jasinge, D., Ranjith, P. G., Choi, S. K., 2011. Effects of Effective Stress Changes on Permeability of Latrobe Valley Brown Coal. *Fuel*, 90(3): 1292–1300. <https://doi.org/10.1016/j.fuel.2010.10.053>
- Lan, F. J., Qin, Y., Li, M., et al., 2012. Abnormal Concentration and Origin of Heavy Hydrocarbon in Upper Permian Coal Seams from Enhong Syncline, Yunnan. *Journal of Earth Science*, 23(6): 842–853. <https://doi.org/10.1007/s12583-012-0294-x>
- Laubach, S. E., Marrett, R. A., Olson, J. E., et al., 1998. Characteristics and Origins of Coal Cleat: A Review. *International Journal of Coal Geology*, 35(1–4): 175–207. [https://doi.org/10.1016/S0166-5162\(97\)00012-8](https://doi.org/10.1016/S0166-5162(97)00012-8)
- Li, G. Z., Sun, F. J., Li, W. Z., et al., 2012. Low-Rank Coalbed Methane Geology of the Northwest China. Petroleum Industry Press, Beijing, 1–20 (in Chinese)
- Li, M., Jiang, B., Lin, S. F., et al., 2013. Structural Controls on Coalbed Methane Reservoirs in Faer Coal Mine, Southwest China. *Journal of Earth Science*, 24(3): 437–448. <https://doi.org/10.1007/s12583-013-0340-3>
- Li, Z. Q., Xian, X. F., Long, Q. M., 2009. Experiment Study of Coal Permeability under Different Temperature and Stress. *Journal of China University of Mining & Technology*, 38(4): 523–527 (in Chinese with English Abstract)
- Liu, C. L., Zhu, J., Che, C. B., et al., 2009. Methodologies and Results of the Latest Assessment of Coalbed Methane Resources in China. *Natural Gas Industry*, 29 (11): 130–132 (in Chinese with English Abstract)
- McKee, C. R., Bumb, A. C., Koenig, R. A., 1988. Stress-Dependent Permeability and Porosity of Coal and Other Geologic Formations. *SPE Formation Evaluation*, 3(1): 81–91. <https://doi.org/10.2118/12858-PA>
- Moosavi, S. A., Goshtasbi, K., Kazemzadeh, E., et al., 2014. Relationship between Porosity and Permeability with Stress Using Pore Volume Compressibility Characteristic of Reservoir Rocks. *Arabian Journal of Geosciences*, 7(1): 231–239. <https://doi.org/10.1007/s12517-012-0760-x>
- Nelson, C. R., Hill, D. G., Pratt, T. J., 2000. Properties of Paleocene Fort Union Formation Canyon Seam Coal at the Triton Federal Coalbed Methane Well Campbell County Wyoming. In SPE/CERI Gas Technology Symposium. Society of Petroleum Engineers, Calgary. <https://doi.org/10.2118/59786-MS>
- Nelson, C. R., 2003. Deep Coalbed Gas Plays in the US Rocky Mountain Region. *Annual Meeting Expanded Abstracts—American Association of Petroleum Geologists*, 12: 127
- Nelson, P. H., Kibler, J. E., 1994. Permeability-Porosity Relationships in Sedimentary Rocks. *The Log Analyst*, 35(3): 38–62
- Niu, S. W., Zhao, Y. S., Hu, Y. Q., 2014. Experimental Investigation of the Temperature and Pore Pressure Effect on Permeability of Lignite under the *in situ* Condition. *Transport in Porous Media*, 101(1): 137–148. <https://doi.org/10.1007/s11242-013-0236-9>
- Olson, T., Hobbs, B., Brooks R., et al., 2002. Paying off for Tom Brown in white River Dom Field's Tight Sandstone and Deep Coals. *The American Oil and Gas Reports*, 10: 67–75
- Palmer, I., 2009. Permeability Changes in Coal: Analytical Modeling. *International Journal of Coal Geology*, 77(1): 119–126, <https://doi.org/10.1016/j.coal.2008.09.006>
- Palmer, I., 2010. The Permeability Factor in Coalbed Methane Well Completions and Production. SPE Western Regional Meeting, Anaheim. <https://doi.org/10.2118/131714-MS>
- Palmer, I., Mansoori, J., 1996. How Permeability Depends on Stress and Pore Pressure in Coalbeds, a New Model. SPE Annual Technical Conference and Exhibition, Denver. <https://doi.org/10.2118/36737-ms>
- Palmer, I., Mansoori, J., 1998. How Permeability Depends on Stress and Pore Pressure in Coalbeds, a New Model. *SPE Reservoir Evaluation and Engineering*, 1(6): 539–544. <https://doi.org/10.2118/52607-PA>
- Pan, Z., Connell, L. D., 2012. Modelling Permeability for Coal Reservoirs: A Review of Analytical Models and Testing Data. *International Journal of Coal Geology*, 92(1): 1–44. <https://doi.org/10.1016/j.coal.2011.12.009>
- Perera, M. S. A., Ranjith, P. G., Choi, S. K., et al., 2012. Investigation of Temperature Effect on Permeability of Naturally Fractured Black Coal for Carbon Dioxide Movement: An Experimental and Numerical Study. *Fuel*, 94: 596–605. <https://doi.org/10.1016/j.fuel.2011.10.026>
- Qin, Y., Fu, X. H., Wei, C. T., et al., 2012. The Dynamic Conditions of the Coalbed Methane and Its Control Effect. Science Press, Beijing, 286–292 (in Chinese)
- Reiss, L. H., 1980. The Reservoir Engineering Aspects of Fractured Formations. Gulf Publishing Company, Houston. 67–77
- Sang, S. X., Qin, Y., Guo, X. B., et al., 2003. Storing Characteristics of Jurassic Coalbed Gas in Junggar and Tuha Basins. *Geological Journal of China Universities*, 9(3): 365–372 (in Chinese with English Abstract)
- Seidle, J. P., Jeansonne, M. W., Erickson, D. J., 1992. Application of Matchstick Geometry to Stress Dependent Permeability in Coals. SPE Rocky Mountain Regional Meeting, Casper. SPE 24361. <https://doi.org/10.2118/24361-MS>
- Shen, J., 2011. CBM-Reservoir Effect in Deep Strata: [Dissertation]. China University of Mining and Technology, Xuzhou (in Chinese with English Abstract)
- Shen, J., Qin, Y., Wang, G. X., et al., 2011. Relative Permeabilities of Gas and Water for Different Rank Coals. *International Journal of Coal Geology*, 86(2): 266–275. <https://doi.org/10.1016/j.coal.2011.03.001>
- Shengli Petroleum Administration Institute of Geological Sciences, 1999. The Porosity and Permeability Measurement of Core in Net Confining Stress, SY/T 6385-1999. State Bureau of Petroleum and Chemical Industry, Beijing. 1–10 (in Chinese)
- Shi, J. Q., Durucan, S., 2004. Drawdown Induced Changes in Permeability of Coalbeds, a New Interpretation of the Reservoir Response to Primary Recovery. *Transport in Porous Media*, 56(1): 1–16. <https://doi.org/10.1023/b:tipm.0000018398.19928.5a>
- Somerton, W. H., Söylemezoglu, I. M., Dudley, R. C., 1975. Effect of Stress on Permeability of Coal. *International Journal of Rock Mechanics and Mining Sciences and Geomechanics Abstracts*, 12(5): 129–145. [https://doi.org/10.1016/0148-9062\(75\)91244-9](https://doi.org/10.1016/0148-9062(75)91244-9)
- Song, Q. Y., 2004. Study on Deep Coalbed Methane Reservoir-Forming Conditions and Its Recovery Potential: [Dissertation]. China University of Mining and Technology, Xuzhou (in Chinese with English Abstract)
- Tang, D. Z., Liu, D. M., Tang, S. H., et al., 2014. Reservoir Dynamic Geological Effect during Coalbed Methane Development Process. Science Press, Beijing. 20–24 (in Chinese)
- Wang, G., Qin, Y., Shen, J., et al., 2014. Experimental Studies and Modeling Analysis of the Deep Low-Rank Coal Reservoirs' Permeability Based on Variable Pore Compressibility. *Acta Petrolei Sinica*, 35(3): 462–468 (in Chinese with English Abstract)
- Yin, G., Jiang, C., Wang, J. G., et al., 2013. Combined Effect of Stress, Pore Pressure and Temperature on Methane Permeability in Anthracite Coal: An Experimental Study. *Transport in Porous Media*, 100(1): 1–16. <https://doi.org/10.1007/s11242-013-0202-6>
- Zhou, Z. Y., Pan, C. C., 1992. Pale Temperature Analysis Methods and Their Application in Sedimentary Basins. Guangzhou Science and Technology Press, Guangzhou. 115–171 (in Chinese)